

Ion Acceleration at Solar Wind Termination Shock

E.G. Berezhko and L.T. Ksenofontov

Yu.G. Shafer Institute of Cosmophysical Research and Aeronomy, 31 Lenin Ave., 677980 Yakutsk, Russia

Presenter: L.T. Ksenofontov (ksenofon@ikfia.ysn.ru), rus-ksenofonov-L-abs1-sh31-poster

Anomalous cosmic ray (ACR) acceleration at the heliospheric termination shock is described by a self-consistent time-dependent kinetic model. Influence of pickup ions injection rate on ACRs spectrum, termination shock structure and its position is investigated. It is shown, that a relatively high injection rate of pickup ions is required to reproduce ACR proton spectrum consistent with the experiment. The termination shock structure and position are quite sensitive to the efficiency of ACR injection/acceleration.

1. Introduction

It is widely believed that the anomalous cosmic rays (ACRs) are the result of heliospheric acceleration of freshly ionized interstellar particles (see review [1]). Interstellar neutral atoms streaming into the solar system are ionized by ultraviolet radiation or by charge exchange with the solar wind and are subsequently accelerated. Diffusive acceleration of some fraction of these pickup ions at the heliospheric termination shock is considered as a main source of ACRs [2]. The detailed model for ACR acceleration at the termination shock should take into account the backreaction of pickup ions and ACRs on the shock structure which is expected to be significant [3, 4, 5].

We develop a time-dependent model that takes into account the selfconsistent interaction of the thermal solar wind plasma, pickup ions and ACRs. The model takes into account the shock modification by the pressure of accelerated particles and can reproduce a selfconsistent spectrum of accelerated particles. It is very similar to the le Roux & Fichtner model [5], but nevertheless our results are essentially different compared with theirs. Opposite to [5] our results demonstrate that the ACR spectrum, shock structure and its position are very sensitive to the injection rate of pickup protons at the termination shock, where some their fraction is presumably involved into the acceleration process. According to our results to reproduce the observed ACR fluxes quite a high injection rate is required.

2. Model

The description of ACR acceleration by a spherical termination shock is based on the diffusive transport equation for the ACR distribution function $f(r, p, t)$:

$$\frac{\partial f}{\partial t} = \frac{1}{r^2} \frac{\partial}{\partial r} r^2 \kappa \frac{\partial f}{\partial r} - w \frac{\partial f}{\partial r} + \frac{1}{r^2} \frac{\partial}{\partial r} (r^2 w) \frac{p}{3} \frac{\partial f}{\partial p} + Q, \quad (1)$$

where $Q = Q_s \delta(r - R_s)$ is the source term due to injection of pickup ions; R_s is the shock radius; r , t and p denote the heliocentric radial distance, the time, and particle momentum, respectively; κ is the radial ACR diffusion coefficient; w is the radial mechanical velocity of the scattering medium (i.e. solar wind plasma). We assume, that the injection of some (small) fraction of pickup ions into the acceleration process takes place at the subshock, which is treated as a discontinuity in our model. For the sake of simplicity we restrict our consideration to protons, which are the dominant pickup ions in the solar wind. At present we only have some experimental and theoretical indications as to what value of the injection rate can be expected. We use here a

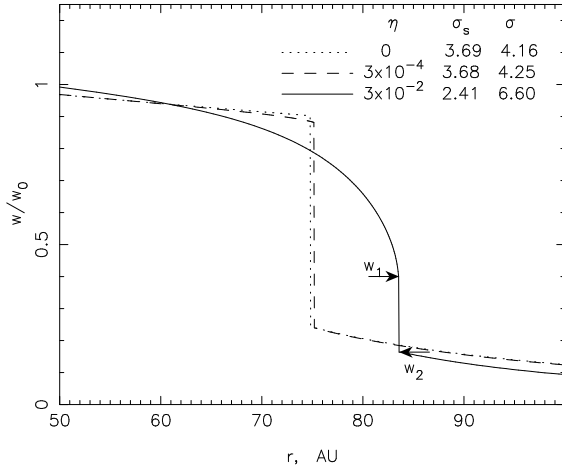


Figure 1. The solar wind speed w as a function of heliospheric distance for high (solid line) and low (dashed) injection rate compared with the solution without ACR ($\eta = 0$, dotted line).

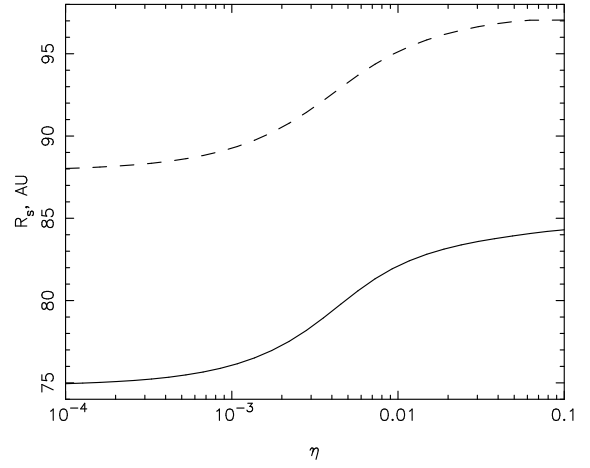


Figure 2. Termination shock radius R_s as a function of pickup ions injection rates η for two different solar wind densities: $n_0 = 5 \text{ cm}^{-3}$ (solid line) and $n_0 = 7 \text{ cm}^{-3}$ (dashed line).

simple injection model, in which a small fraction η of the incoming pickup protons is instantly injected at the gas subshock with a speed $\lambda > 1$ times the postshock gas sound speed c_{s2} :

$$Q_s = \frac{u_1 N_{inj}}{4\pi p_{inj}^2} \delta(p - p_{inj}), \quad N_{inj} = \eta N_1^{pu}, \quad p_{inj} = \lambda m c_{s2}, \quad (2)$$

where $u = w - V_s$, $V_s = dR_s/dt$ is the shock speed, N^{pu} is the number density of pickup protons, and m is the proton mass. An appropriate value $\lambda = 4$ [6] is used here. The subscripts 1(2) refer to the point just ahead (behind) the subshock.

We use the ACR diffusion coefficient

$$\kappa(p) = 6 \times 10^{20} (p/mc)(v/c)(50 \mu\text{G}/B) \text{ cm}^2/\text{s}, \quad (3)$$

where v is particle velocity, c is the speed of light, B is magnetic field strength. In the vicinity of the termination shock, that is at $|r - R_s| \ll R_s$, this coefficient coincides with that which was assumed in [5], whereas at smaller distances $r \ll R_s$ it is significantly smaller. Therefore the ACR spectra at the shock front are expected to be very similar in these two models, whereas at smaller distances $r \ll R_s$ ACR fluxes are expected to be progressively lower compared with their model. Note that opposite to [5] we do not take into account the influence of the galactic cosmic rays on the shock structure. This difference between two models is not very essential, because galactic cosmic ray influence is not significant [5].

The velocity profile $w(r, t)$ and pickup proton distribution $N^{pu}(r, t)$ are selfconsistently computed from a system of gas dynamic equations which include the ACR pressure P_c and the source and loss terms which describe the production of pickup protons resulting from photoionization of, and charge exchange with, interstellar hydrogen in the same form as in [5] (see [7] for the details). The above equations are solved numerically with the boundary conditions at $r_0 = 1 \text{ AU}$ (medium speed $w_0 = 400 \text{ km/s}$, number density $n_0 = 5 \text{ cm}^{-3}$ and temperature $T_0 = 10^5 \text{ K}$) and at $r = \infty$ (medium speed $w = 0$ and pressure $P = P_{ISM} = 1 \text{ eV/cm}^3$). Note, that the value $n_0 = 5 \text{ cm}^{-3}$ used in [5] underestimates the typical solar wind density. Therefore in Fig. 2 and 3 we also present results of calculations with the typical value $n_0 = 7 \text{ cm}^{-3}$.

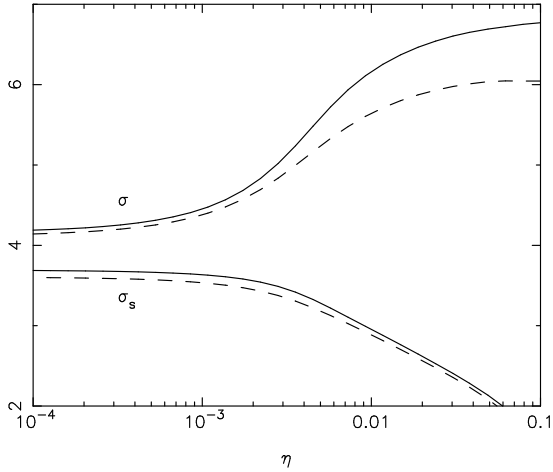


Figure 3. The total compression ratio of termination shock σ and subshock compression ratio σ_s as a function of pickup ions injection rates η for the same cases as in Fig. 2.

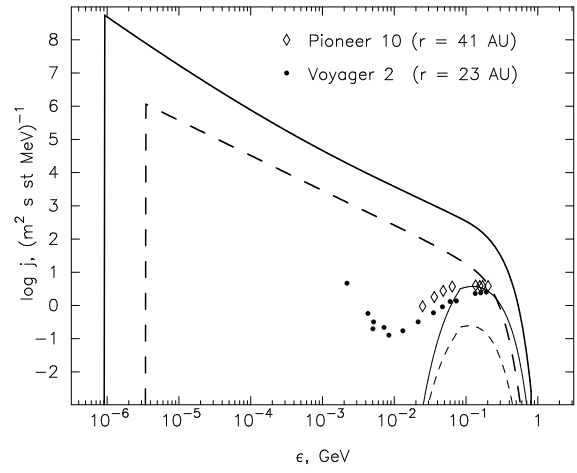


Figure 4. Differential ACR intensity as a function of kinetic energy for high ($\eta = 3 \times 10^{-2}$, solid lines) and low ($\eta = 3 \times 10^{-4}$, dashed lines) injection rates. Thick and thin lines correspond to $r = R_s$ and $r = 30$ AU respectively. Experimental data measured at $r = 23$ AU and 41 AU are shown [11].

3. Results and Conclusions

We analyze here the steady state of the system which is established during the time interval of a few years after the beginning of pickup proton injection/acceleration. Results of calculations are shown in Figs. 1–4. Since the actual injection rate of pickup protons is not known we present the calculations which correspond to the low ($\eta = 3 \times 10^{-4}$) and high ($\eta = 3 \times 10^{-2}$) injection rates.

The solar wind velocity profile $w(r)$, shown in Fig. 1, consists of a pure gas subshock at $r = R_s$ and extended smooth precursor originated in the upstream region $r < R_s$ due to the influence of pickup ions and ACRs. The solution without ACRs, that formally means $\eta = 0$, corresponds to the shock radius $R_s = 74.9$ AU, shock compression ratio $\sigma = w_0/w_2 = 4.16$ and subshock compression ratio $\sigma_s = w_1/w_2 = 3.69$. At low injection rate $\eta = 3 \times 10^{-4}$ these shock parameters are almost the same (see Fig. 1). In these case our values of the shock parameters are close to those obtained in [5], which are $R_s = 75.1$ AU, $\sigma_s = 3.68$ and $\sigma = 4.25$. The increase of the injection rate leads to higher shock modification due to ACR backreaction, that is larger shock compression ratio and weaker subshock. The increase of the shock compression provides the increase of the postshock pressure that in turn shifts the shock position towards larger distance r . In the case of $\eta = 3 \times 10^{-2}$ shown in Fig. 1 we have $R_s = 84$ AU, $\sigma = 6.6$ and $\sigma_s = 2.4$. Surprisingly that the solution obtained in [5] at high injection rate is essentially different. Opposite to what is expected from general point of view at higher η they have smaller shock radius R_s and lower shock compression ratio σ .

As it is seen in Fig. 2, the shock size R_s increases on the value $\Delta R_s \simeq 10$ AU due to the increase of the injection rate η from the low ($\eta \lesssim 10^{-3}$) to high ($\eta \gtrsim 10^{-2}$) values. The expected range of the shock sizes at the realistic solar wind density $n_0 = 7 \text{ cm}^{-3}$ lies within the range $R_s = 88 - 97$ AU, that very well corresponds to the recently detected by Voyager 1 termination shock sizes [8]. The significant influence of ACR on the shock size R_s (Fig. 2) is in qualitative agreement with the results obtained in [9, 10].

The degree of the shock modification due to ACR backreaction is also very sensitive to the injection rate η . As it seen from Fig. 3 the total shock compression ratio σ monotonically increases and the subshock compression ratio σ_s decreases with increase of η . At the most appropriate value of the injection rate $\eta \sim 10^{-2}$ we have $\sigma \approx 6$ and $\sigma_s \approx 3$.

Fig. 4 shows the differential ACR intensity $j = p^2 f$ as function of kinetic energy ϵ_k at $r = R_s$ and $r = 30$ AU. One can see that the shape of ACR spectra are essentially different for different η . At energies $\epsilon_k \sim 100$ MeV, which is the typical ACR energy, the flux value at low injection is more than two orders of magnitude smaller than at high injection. It is also clear from Fig.1 that relatively high injection rate $\eta \sim 10^{-2}$ is required to reproduce the observed ACR fluxes at $r = 23 \div 41$ AU. Note that the solutions obtained in [5] due to unknown reasons are dramatically different: their ACR spectra are almost insensitive to the injection rate except very low energy range.

Thus our preliminary calculations demonstrate that opposite to the previous study [5] the ACR spectrum, produced as a result of the diffusive acceleration of some part of pickup protons, the termination shock structure and its position are very sensitive to the pickup proton injection rate. Quite a high injection rate $\eta \sim 10^{-2}$ is required to reproduce observed ACR fluxes.

This work has been supported by the INTAS grant WP 0270, by the Russian Foundation for Basic Research (grant 03-02-16325) and by LSS grant 422.2003.2.

References

- [1] H. Fichtner, Space. Sci. Rev. 95, 639 (2001).
- [2] M.E. Pesses, J.R. Jokipii, D. Eichler, ApJ 246, L85 (1981).
- [3] J.R. Jokipii, Physics of the Outer Heliosphere (ed. S.Grzedzielski, D.E.Page, Pergamon, 1990, p.169).
- [4] D.J. Donohue, G.P. Zank, J.Geophys.Res. 98, 19005 (1993).
- [5] J.A. le Roux, H. Fichtner, ApJ 477, L115 (1997).
- [6] E.G. Berezhko, D.C. Ellison, ApJ 526, 385 (1999).
- [7] E.G. Berezhko, L.T. Ksenofontov, Proc. 28th ICRC, Tsukuba, 3761 (2003).
- [8] S.M. Krimigis, R.B. Decker, M.E. Hill, et al. Nature 426, 45 (2003).
- [9] D.B. Alexashov, S.V. Chalov, A.V. Myasnikov, V.V. Izmodenov, R. Kallenbach, A&A 420, 729 (2004).
- [10] V. Florinski, G.P. Zank, J.R. Jokipi, E.C. Stone, A.C. Cummings, ApJ 610, 1169 (2004).
- [11] F.B. McDonald, A. Lukasiak, W.R. Webber, ApJ 446, L101 (1995).